

UNCLASSIFIED

AD 407 567

DEFENSE DOCUMENTATION CENTER

FOR

SCIENTIFIC AND TECHNICAL INFORMATION

CAMERON STATION, ALEXANDRIA, VIRGINIA



UNCLASSIFIED

NOTICE: When government or other drawings, specifications or other data are used for any purpose other than in connection with a definitely related government procurement operation, the U. S. Government thereby incurs no responsibility, nor any obligation whatsoever; and the fact that the Government may have formulated, furnished, or in any way supplied the said drawings, specifications, or other data is not to be regarded by implication or otherwise as in any manner licensing the holder or any other person or corporation, or conveying any rights or permission to manufacture, use or sell any patented invention that may in any way be related thereto.

407567

AD No.

DDC FILE COPY

AFOSR 4631

(4) \$3.60

(5) 16 600

(20) 11

(21) NA

63-4-1

(6) Electron-Ion Reaction Rate Theory. Determination of the Properties of Non-Equilibrium Plasmas in MHD Generators and Accelerators and in Shock Tubes,* (7)-(9) NA

(10) by
STANLEY BYRON, PAUL I. BORTZ AND GARY R. RUSSELL**
Aeronutronic, Division of Ford Motor Co.
Ford Road, Newport Beach, Calif.

(11) [1963] (12) [33] p. (13) - (14) NA people-3

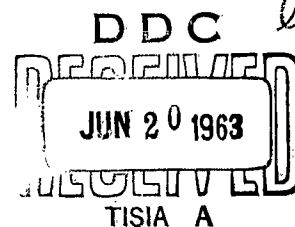
ABSTRACT

The theoretical analysis required to determine the electron density, electron temperature, excited state populations and radiation emission of monatomic plasmas is described. Available information on inelastic cross-sections and radiative emission and absorption is reviewed. The range of physical parameters over which various non-equilibrium effects are significant is examined. Examples of the application of this theory to the non-equilibrium magnetohydrodynamic generator, the crossed-field accelerator and the shock tube are presented.

(15)
*Supported in part by the Air Force Office of Scientific Research
under Contract AF 49(638)670.

**Now at Jet Propulsion Laboratory, Pasadena, California.

\$3.60



Introduction

In magnetohydrodynamics it is often found that equilibrium gas properties are inadequate in describing the true behavior of the gas. Unfortunately no simple prescription has been evolved which, when applied to a given set of experimental conditions, determines unambiguously whether or not the gas is in equilibrium. In this paper a summary of current information on the non-equilibrium properties of partially ionized monatomic gases is given from which a rather complex prescription can be formulated.

If one or more of the following criteria are met the gas can be said to be out of equilibrium:

1. The electron-ion-neutral reaction time is of the same order as or longer than any other time characteristic of the problem.
2. The net radiation decay rate of any of the excited states is of the same order as or greater than the net collisional rate of populating that excited state.
3. The electron temperature is significantly different from the atom and ion temperature.

The discussion of these restrictions is limited to monatomic gases because of the absence of the additional complications found in molecular gases (rotation, vibration, dissociation, etc.) and also because only for monatomic gases is there sufficient information on collision cross-sections at the present time to make use of these criteria.

It has been established previously⁶ that electronic excitation and de-excitation occur primarily by electron impact with atoms and by

radiative emission and absorption. Other processes such as dissociative recombination and atom impact excitation do occur, but they are insignificant in monatomic gases when the electron mole fraction is greater than 10^{-5} to 10^{-6} .

A semi-classical method for computing electron impact excitation and de-excitation cross-sections has been developed recently by Gryzinski.¹ In his original paper Gryzinski shows that the theory agrees well with measurements of several specific excitations and ionization cross-sections. The theory has been used by Bates, et.al.^{7,8} and by Byron, et.al.⁹ to obtain integrated excitation and de-excitation cross-sections for hydrogen-like atoms. Combining these cross-sections with available radiative de-excitation probabilities¹⁰ and with the electron energy equation,²³ an electron-ion recombination theory has been formulated for hydrogen and helium.⁹ This is found to be in good agreement with experimental measurements in helium.^{8,11}

In the following, an approximation to Gryzinski's method is used to compute cross-sections for electronic transitions in argon and potassium in the temperature range between 500°K and 2000°K . Coupling these with radiative emission and absorption probabilities, the rate of electron-ion recombination is determined in this temperature range. The rate is applied to the problem of producing non-thermal ionization in a non-equilibrium mhd generator. Application of the electron energy transfer equation to the problem of producing non-equilibrium thermal ionization in mhd generators is also discussed. The influence of radiation on electron temperature, population of the excited states, and electron density under quasi-steady conditions is described. Finally, a summary is given of the application of

the reaction rate equations and the two-fluid gasdynamic flow equations to compute the electron density, electron temperature, and the electrical conductivity in a supersonic nozzle expansion and in a crossed field mhd accelerator.¹²

Electronic Transitions by Electron Impact

According to the theory of Gryzinski,¹ his equation (28) is used in computing the cross-section for collisional excitation of the level having binding energy E_1 , to that having binding energy $E_1 - U_1$, when the next higher excited state has a binding energy $E_1 - U_2$. The cross-section as a function of electron energy, E_2 , is then integrated over a Maxwell distribution of electron energies. The result for hydrogen is given in analytic form in Ref. 9 and shown graphically here in Fig. 3 as a function of excited state binding energy, E^* . The result for excited states of helium in the binding energy range shown in Fig. 3 is approximately twice that of hydrogen.

For more complex atoms such as argon and potassium, a great number of cross-sections must be computed and summed to obtain exact results. Noting that the cross-section is inversely proportional to the square of the energy gap, U , between the initial and final excited states (Eq. 23 and 26 of Ref. 1) an approximation is immediately suggested. From the table of atomic energy levels, the larger energy gaps may be selected. It is found that the energy gaps adjacent to the large gap, U , are considerably smaller than U . This justifies using the approximation that the energy levels above and below the gap are continuous. It is also found that these closely spaced energy levels extend over an energy range greater than U both above

and below the gap. Therefore if the electron thermal energy is of the order of or less than the gap energy, U , Eq. 26, Ref. 1 is a good approximation to Eq. 28, Ref. 1 in computing g_j as a function of electron energy.

The factor $g_j(E_2/U; E_1/U)$ found in eq. 26 and 27 for this case ($U + E_1 < E_2$) is reproduced here in Fig. 1, where E_1 is the kinetic energy of the bound electron (the same as the binding energy for a single excited electron), U the energy gap, and E_2 the kinetic energy of the impacting electron. It is seen that a linear approximation to g_j vs E_2/U , which greatly simplifies the subsequent integration over a Maxwell distribution of electron energies, reproduces g_j within 30% over the range $1 + .005 E_1/U \leq E_2/U \leq 2 + .1 E_1/U$. If we make the assumption that kT_e lies in the range $.01 E_1 \leq kT_e \leq U + .1 E_1$, the linear approximation is valid. For example, if the binding energy is 1 ev and the gap energy is 0.2 ev, the linear approximation is valid for electron temperatures between 116°K and 3480°K. The integrated cross-section for excitation of level E_1 to $E_1 + U$ or higher is then given by

$$\bar{\sigma}_c \Big|_u = \int_u^\infty Q(u) c f c^2 dc / \int_0^\infty f c^2 dc = \sqrt{\frac{5kT_e}{\pi m_e}} \frac{\sigma_0 B}{U^2} \left[1 + \frac{2kT_e}{U^2} \right] e^{-U/kT_e} \quad (1)$$

where σ is the collision cross section (cm^2), c the electron speed (cm/sec), $Q(U)$ is obtained from eq. (26), Ref. 1, f is the Maxwell distribution function, σ_0 is $6.56 \times 10^{-14} \text{ cm}^2 - (\text{electron volt})^2$, B is the slope of the linear approximation to g_j , U is the gap energy (electron volts), k is Boltzmann's constant, and T_e and m_e are the electron temperature and mass. The slope, B , as a function of E_1/U is reproduced in Fig. 2.

The cross-section given in eq. 1 is for a transition from a particular state having binding energy E_1 to any state having binding energy less than or equal to $E_1 - U$. The total rate of crossing the energy gap U in the upward direction is actually given by the sum of the contributions from E_1 and all levels below E_1 . Using the approximation that the levels below E_1 are continuous, the total rate of crossing U is

$$\begin{aligned} \left. \frac{dN_e}{dt} \right|_u &= \frac{N_1}{g_1} \sqrt{\frac{8kT_e}{\pi m_e}} \sigma_e B \int_0^\infty \frac{[1 + 2kT_e/(u+E)]}{(u+E)^2} e^{-(u+E)/kT_e} g e^{+E/kT_e} dE \\ &= \sqrt{\frac{8kT_e}{\pi m_e}} \frac{\sigma_e B}{u^2} \left(1 + \frac{kT_e}{u}\right) e^{-u/kT_e} N_e N_1 \frac{g u}{g_1} \end{aligned} \quad (2)$$

where N_1 and g_1 are the number density and degeneracy of the states having binding energy E_1 , and g is the average degeneracy per unit energy interval over the interval U below E_1 .

Using the principle of detailed balancing and the approximation of continuous levels in the range kT_e above that having a binding energy, $E^* = E_1 - U$, the de-excitation cross-section from all levels above E^* and the rate of crossing the gap U in the downward direction are given by

$$\sigma_c \Big|_d = \sqrt{\frac{8kT_e}{\pi m_e}} \frac{\sigma_e B}{u^2} \left(1 + \frac{kT_e}{u}\right) \quad (3)$$

$$\left. \frac{dN}{dt} \right|_d = \sqrt{\frac{8kT_e}{\pi m_e}} \frac{\sigma_e B}{u^2} \left(1 + \frac{kT_e}{u}\right) N_e N_2 \frac{g u}{g_2} \quad (4)$$

where N_2 and g_2 are the number density and degeneracy of atoms having binding energy E^* and gU is the total degeneracy of states having binding energy between E^* and $E^* - U$. At equilibrium N_2 is related to the free electron density by

$$N_2 = \frac{g_2}{g_e g_i} \left(\frac{h^2}{2\pi m_e k T_e} \right)^{3/2} e^{+E^*/kT_e} N_e^2 \quad (5)$$

where h is planck's constant and g_e and g_i are the degeneracy of the free electron and the ion.

The product $\bar{\sigma}c$ has been determined for argon and potassium, using values for U , E_1 , and E^* derived from NBS tables.¹³ The results are shown graphically in Fig. 3. Note that these cross-sections are unusually large ranging between 10^{-13} and 10^{-10} cm^2 .

The equilibrium collisional de-excitation rate, eqs. (4) and (5), normalized by the cube of the electron density, is shown graphically in Fig. 4 for hydrogen, potassium, and argon at three electron temperatures. Note that there is a minimum equilibrium de-excitation rate for each gas at each electron temperature. As described previously⁹ the equilibrium rate of de-excitation at the minimum point determines the net rate of electron-ion recombination, the ratio of the latter to the former being a factor, γ , which varies between 1 and 1/4 (see Ref. 9). For this temperature range, $\gamma \approx 1/3$.

The resulting electron-ion recombination rate coefficient $N_e^{-3} dN_e/dt$, for argon, potassium, and hydrogen is shown graphically as a function of electron temperature in Fig. 5. Over this temperature range the rate for helium is approximately four times that for hydrogen. It is seen that the rate for potassium, a hydrogen-like atom, falls within a factor of 2 of that for hydrogen, whereas the rate for argon, an atom having very closely spaced excited states, is an order of magnitude larger than that for hydrogen over quite a wide range of temperature. Note also that the recombination rate changes very steeply with electron temperature in this range.

Radiation

At low electron densities radiative transitions contribute significantly to the recombination rate. Also, it has been shown that under steady state conditions radiation shifts the distribution of excited states away from the equilibrium distribution and may lower the electron density considerably below the Saha equilibrium value.⁷

The spontaneous emission probabilities for hydrogen are found in Refs. 10 and 14. Values for helium are very close to those for hydrogen except for low lying excited states, which are given in Ref. 15. Few values for other gases such as potassium and argon are available.

The inclusion of radiation in the ionization and recombination theory has been done for optically thin hydrogen exactly by Bates, et.al.⁷ and approximately by Byron, et.al.⁹ It has also been done for optically thick hydrogen by Bates, et.al.⁸ The resulting recombination rate coefficients for the optically thin case⁹ are shown in Fig. 5 for hydrogen with $N_e = 10^{10}$ and 10^{12} cm^{-3} . The recombination rate coefficients given here for hydrogen are as much as a factor of two smaller than those given by Bates,⁷ probably because of the simplifying approximations that are used.⁹

In order to make physically realistic computations which include radiative effects it is necessary to include the effect of re-absorption. This can be done in a general way by considering three distinct possibilities: (1) the gas is optically thick only for transitions from excited states to the ground state, (2) it is optically thick for all line radiation, and

(3) it is optically thick for all line and continuum radiation. Which of these models if any applies to a particular physical situation depends on each of the absorption coefficients.

The absorption coefficient, α_ν (cm^2), of an atomic line is determined by the oscillator strength, f , of the line and the line shape. Only the strong transitions ($f \approx 1$) need to be considered since these dominate the effect of radiation on excited state populations. The line shape is discussed extensively in the astrophysics literature¹⁶ and is thoroughly reviewed in a recent article by Baranger.¹⁷ The principal sources of broadening of atomic lines in partially ionized gases of interest here are Doppler broadening and pressure broadening.

Doppler broadening alone can be treated rather simply,¹⁶ yielding the result that the line width, $\Delta\nu_0$ (sec^{-1}), and the absorption coefficient at line center are given by

$$\Delta\nu_0 = \sqrt{2kT/M} \nu_0/c \quad ; \quad \alpha_c = \sqrt{\pi} e^2 f / mc \Delta\nu_0 \quad (6)$$

where ν_0 is the line frequency, M the atom mass, c the speed of light, m the electron mass, and other symbols have been defined previously. The absorption at line center is significant here because emission at line center contributes most to changes in excited state populations. The value of $\Delta\nu_0 / \nu_0$ for plasma temperatures between 1000°K and $20,000^\circ\text{K}$ ranges from 3×10^{-5} for low molecular weight gases to 10^{-6} for heavy gases and low temperatures. Using $f \approx 1$, α_0 ranges from $500/\nu_0$ to $1.7 \times 10^4/\nu_0$. Now the optical depth may be computed if the number density of absorbing atoms is known. Using an optical depth of 1 cm as the division between optically thick and optically thin problems, the division occurs when the density of the lower state is in the range $\nu_0/500$ to $\nu_0/1.7 \times 10^4$,

or 5×10^{12} to $1.5 \times 10^{11} \text{ cm}^{-3}$ for 10 ev photons. Since the ground state population in magnetohydrodynamic devices is usually greater than these limits, the gas is optically thick for transitions from an upper state to the ground state.

The excited state populations (eq. 5) are of the order of $10^{-18} N_e^2$ and the emission frequencies for which the lower level is an excited state fall in the range 1 to 4 ev. Therefore in general the gas is optically thin for transitions from one excited state to another if $N_e \leq 10^{14} \text{ cm}^{-3}$, whereas it is optically thick for these transitions if $N_e \geq 10^{15} \text{ cm}^{-3}$. More definitive limits than these can be set only by examining each physical situation in detail.

Pressure broadening exceeds Doppler broadening of low excited states at electron densities of the order of 10^{15} cm^{-3} , and lower for higher states.¹⁷ Techniques are now available^{17,18} which can be used to compute the broadening of hydrogen and non-hydrogen atoms, but few specific examples have been carried out. Considerable work in the future is required before there will be sufficient information on line broadening and absorption to allow accurate quantitative computations of the effect of radiation on gas properties.

It should be pointed out here that molecular band emission covers a much broader wavelength region than does atomic line emission. Because of this the absorption coefficient is much lower for molecular emission and the lower state population required to produce an optical depth of 1 cm is of the order of 10^{16} cm^{-3} . Thus molecular band emission is generally optically thin.

The free-free and free-bound continuum radiation from argon has been treated theoretically by Pomerantz¹⁷ and studied experimentally by Olsen.²⁰ From these results it is found that an absorption length of 1 cm for the continuum in the visible range is obtained when the electron density is of the order of 10^{18} cm^{-3} . Since in mhd devices the electron density is usually much smaller than 10^{18} cm^{-3} , the gas is transparent to continuum radiation.

Returning to the three classes of absorption described above, it can be said in general that the gas in mhd devices is optically thick for transitions from excited states to the ground state, optically thin for continuum radiation, and the optical depth for transitions from one excited state to another may be of the order of 1 cm and must be computed for the particular operating conditions.

Non-Equilibrium MHD Generator

The electron-ion recombination rates shown in Fig. 5 can be used to investigate the concept of non-thermal ionization in mhd generators.⁴ Because mhd generators operate efficiently at pressures of the order of 1 atmosphere or greater, electron densities must be of the order of 10^{14} cm^{-3} or greater in order to reach high electrical conductivity. At these electron densities and in the temperature range typical of mhd generators radiation can be neglected in computing the recombination rate (see Fig. 5). It is important to note that the collisional recombination reaction behaves like a three-body process, the rate being proportional to the cube of the electron density, not to the square of the electron density as is often assumed.

The electrical power density output of a segmented electrode generator is

$$P_{gen} = .25 \sigma U^2 B^2$$

where the load factor is taken as 1/2, σ is the scalar gas conductivity, U the flow velocity, and B the applied magnetic field strength. In designing a generator the magnetic field strength is chosen to produce a particular operating value of the Hall parameter, $\mathcal{N} = \omega \tau$, such that $B = \mathcal{N} m / \tau e$, where ω is the electron cyclotron frequency, and τ is the mean time between collisions of electrons with heavy particles. τ is given by $\tau = (N_a (Q\bar{c}))^{-1}$ where N_a and Q are the number density and collision cross-section for the heavy particle that dominates momentum transfer collisions with electrons, and \bar{c} is the electron mean speed. Then

$$P_{gen} = .25 \sigma U^2 (\mathcal{N} m N_a Q \bar{c} / e)^2 \quad (7)$$

The energy required to replace the electrons lost by recombination is of the order of

$$P_{loss} = -E_{ion} dN_e/dt = E_{ion} \beta N_e^3 \quad (7)$$

where E_{ion} is the ionization potential for the predominant ion. If it is assumed that $P_{loss} \leq 0.1 P_{gen}$ for efficient operation, a limitation on the operating region is given by the inequality

$$E_{ion} \beta N_e^3 \leq .025 \sigma U^2 (\mathcal{N} m N_a Q \bar{c} / e)^2 \quad (8)$$

Evidently a high flow velocity and high Hall parameter are favorable whereas a high atom density is unfavorable because it must be accompanied by a high electron density if electrical conductivity is not to be sacrificed.

As an example, helium at a stagnation temperature of 1800°K , operating at $M_1 = 0.8$, $T = 1482^{\circ}\text{K}$, $U = 2300$ m/sec, $K = 5$, $N_a = 3 \times 10^{18} \text{ cm}^{-3}$, is chosen. The electron neutral cross-section is $5.7 \times 10^{-16} \text{ cm}^2$ for helium.²¹ To approach Spitzer conductivity the electron density must be $3.8 \times 10^{14} \text{ cm}^{-3}$. At the operating temperature $\beta = 9 \times 10^{-23} \text{ cm}^6/\text{sec}$ for helium (four times that for hydrogen, see Fig. 5). Using these values, the loss rate on the left of eq. 8 exceeds the allowed supply rate on the right by a factor of 2000. One operating point which meets the restriction of eq. 8 is that at an electron density that is lower by a factor of $\sqrt{2000}$, or a value of $8.4 \times 10^{12} \text{ cm}^{-3}$, but this yields an electrical conductivity of only 0.049 mhd/cm. This particular example does not appear attractive for practical mhd power generation. Further detailed analysis may yield more attractive operating conditions.

The difficulty encountered here can be eliminated by operating at lower pressures and higher stagnation temperatures. Some improvement is to be found using different gases, for example, a potassium additive to helium which lowers E_{ion} by a factor of 5 and β by a factor of 2. The use of some other noble gas such as argon with its high recombination coefficient is disadvantageous.

An interesting possibility is that the recombination process heats the electrons to a temperature substantially higher than that of the gas. This reduces the recombination rate to the point at which the

recombination energy is equal to the energy transferred by elastic collisions to heavy particles. The rate of transfer of energy from electrons to ions and neutrals is given by

$$Q_{el} = 3k(T_e - T_a) \frac{m_e}{m_i} N_e \bar{c} (N_e Q_{ei} + N_a Q_{en}) \quad (9)$$

For the conditions described above (and assuming that radiation losses are unimportant) the electron temperature would be increased to 3900°K , reducing the energy loss rate to 5 times that of the electrical power density output.

Operating in this manner the "non-thermal ionization" mhd generator is distinguished from the "non-equilibrium ionization" generator³ only by the manner in which the electrons are heated. Joule heating by the induced current is used in the latter, whereas an electron beam or some other external source may be used in the former.

Electron heating in non-equilibrium mhd generators has been examined in some detail.^{2,3,5,26} It should be noted, however, that a mistaken impression concerning the limits of the mean loss factor, δ , may be inferred from Ref. 3. Following eq. (13) it is stated that "The maximum value of T_e/T_0 is $5/3$, corresponding to $\delta = 1$, $K = 0$, and $\gamma = 5/3$ ", giving the impression that the minimum value of δ is 1. However, if a small amount of a high molecular weight easily ionized gas is used with a low molecular weight gas having a small electron-neutral cross-section, δ may be much less than 1.

If two components are chosen for the working fluid, the mixture ratio that minimizes δ is easily determined by setting the derivative of eq. (1) of Ref. 3 equal to zero, yielding the results

$$\frac{M_2}{M_1} = \sqrt{\frac{Q_2}{Q_1}} \quad ; \quad X_2 = \left(\sqrt{\frac{Q_2}{Q_1}} - 1 \right) / \left(\frac{Q_2}{Q_1} - 1 \right)$$

$$\delta_{opt} = 4 \sqrt{\frac{Q_2}{Q_1}} \left(\frac{\sqrt{\frac{Q_2}{Q_1}} - 1}{\frac{Q_2}{Q_1} - 1} \right)^2 \quad (10)$$

where M is the molecular weight, Q the cross-section, X the mole fraction, and the subscript 2 represents the heavy, large cross-section component of the gas. For $Q_2/Q_1 = 2000$ which is roughly the ratio of the Coulomb cross-section of cesium to the electron-neutral cross-section of helium, the optimum mass ratio is 45, also close to that for cesium and helium. The optimum mole fraction of cesium ion is 2.2%, and the loss factor, δ , under these conditions is 0.09. Using eq. 15, Ref. 3, the ratio of electron temperature to stagnation temperature is equal to 4.1 for a segmented electrode generator operating with this mixture at $M = 0.8$, $K = 0.5$, $\omega_e \tau_e = 2$.

To summarize this section, calculated values of the electron-ion recombination rate are so high that "non-thermal ionization" for mhd power generation is probably not practical. On the other hand, elevation of the electron temperature either by Joule heating or by external methods or both appears quite practical, particularly when applied to mixtures of light neutrals with heavy ions.

QUASI-STEADY EFFECTS

Of the non-equilibrium criteria given in the introduction, an example of the first was discussed in the preceding section. The second and third are discussed in this section. For optically thin hydrogenic atoms under quasi-steady conditions, it has been shown⁷ that a significant reduction in the populations of the excited states and the electron density below the equilibrium values based on statistical mechanics using the local value of the electron temperature may be caused by radiation from the excited states. This reduction is significant if the net radiative de-excitation probability of an excited state is of the order of or larger than the net collisional probability of exciting the state. Application of this criterion in practice requires knowledge of the collisional excitation cross-sections, the radiative decay probabilities, and the absorption coefficients. To see the range of physical parameters for which this effect is important, hydrogen-like atoms subject only to Doppler broadening will be examined.

For optically thin hydrogen the collisional de-excitation probability equals the radiative de-excitation probability of an excited state having principal quantum number n when⁹

$$166 \times 10^8 / n^{4.5} \approx 1 \times 10^{-8} (n-1)^5 N_e \quad (11)$$

From this we can compute the electron density below which the population of level n may differ appreciably from equilibrium. The collisional de-excitation probability of the level n is used here because at equilibrium it is the same as the probability of collisional excitation of the level n .

From the preceding discussion of radiation, the population of the lower state below which a sample of gas 1 cm thick is optically thin is given by $N_p = 1/\alpha_0$. The absorption coefficient, α_0 , is given in

terms of the line width, $\Delta \nu_0$, which is a function of the emission frequency, ν_0 . Only the emission from a level n to the next lower level will be considered for hydrogen, as it is assumed that the gas temperature is so low that if radiation to the next lower level is absorbed, emission to all levels is absorbed. Then $\nu_0 = R_y [(n-1)^{-2} - n^{-2}] / h$ where R_y is the Rydberg constant. The limit, N_l , is then given by

$$N_l = \sqrt{\frac{2kT}{\pi M}} \frac{m R_y}{h e^2} [(n-1)^{-2} - n^{-2}] \quad (12)$$

At equilibrium, the population of the level $n - 1$, N_{l-1} , is related to the electron density by eq. 5. Then eq. 12 yields an upper limit to N_e , above which radiation from level n is self-absorbed. Eq. 11 yields a lower limit to N_e , below which radiation causes the population of level n to be out of equilibrium. Then for each gas temperature a level n_c can be found at which these two restrictions to N_e give the same result. It can then be seen that if the electron density is above the value given by eq. 11 using the value of n_c computed from eqs. 11, 12, and 5, all of the excited states will be nearly in equilibrium. For levels below n_c the radiation is trapped. For levels above n_c , the collisional excitation rate is greater than the optically thin radiative de-excitation rate. These limiting values of n_c and N_e are tabulated below as a function of T_e .

Table I: Electron densities below which non-equilibrium steady-state populations of the excited states n_c and below may occur for hydrogenic atoms

n_c	2	3	4	5
$T_e (^{\circ}\text{K})$	43,500	5600	1830	850
$N_e (\text{cm}^{-3})$	3.7×10^{16}	1.8×10^{14}	8×10^{12}	8×10^{11}

The effect of pressure broadening, which has not been included in computing Table I, will be to lower the temperatures at which the limiting values of N_e given in Table 1 occur. It can be seen that many experimental situations arise which lead to non-equilibrium steady state populations for hydrogen. For other gases the Doppler line broadening is less and the energy levels are more closely spaced, both of which lower the limiting values of N_e .

In order to compute the gas properties, such as the electron density and the radiation emission, under conditions that lead to non-equilibrium excited state populations, it is necessary to solve the set of equations that includes the rate of populating and depopulating each level up to a level which is in equilibrium with the free electron density, thus terminating the set of equations with eq. 5. This is closely related to the theoretical model used by Ben Daniel^{5,26} to determine the effect of Joule heating of electrons on electrical conductivity.

This brings us to the third non-equilibrium effect mentioned in the introduction. The electron temperature may differ from the atom temperature, even after the gas relaxes to a quasi-steady value, if processes in the gas supply or absorb thermal energy of the electrons more rapidly than it can be transferred from electrons to ions and neutrals. The following discussion will be focused on the effect of radiation on the electron temperature, in the absence of electric and magnetic fields. This will serve to delineate the regions in which the effect of radiation must be included in determining the electron temperature.

For this purpose radiation can be divided conveniently into free-free plus free-bound continuum radiation and atomic line radiation, each treated separately. The electrons are cooled because the depletion of excited states and free electrons caused by radiative transitions is replenished by inelastic collisional excitation and ionization by electron impact. This results in a lowering of the electron temperature to a value which produces a balance between the inelastic energy loss rate (equal to the radiation loss rate) and the elastic energy transfer rate between electrons and heavy particles.

The continuum radiation is proportional to the square of the electron density,^{19,22} as is the rate of transfer of energy from electrons to ions.²³ Since the former is independent of ion mass and the latter inversely proportional to ion mass, the largest temperature difference is expected for the heaviest ions. In the event that elastic energy transfer from neutrals to electrons is dominant, the temperature difference will be smaller than that computed on the assumption that ion-electron elastic energy transfer is dominant. If this is done by equating the total continuum radiation²² to eq. 11, Ref. 23, the electron temperature is given by

$$\left(\frac{T_a}{T_e} - 1\right) = \frac{16 \pi e^2 m_i \Delta \nu \exp(1)}{3 \sqrt{3} m_e^2 c^3 \ln \left[q(k T_e)^3 / 8 \pi N_e e^6 \right]} \quad (13)$$

where $\Delta \nu$ is the frequency range over which the continuum extends. There is recent experimental evidence²⁰ that the Unsold theory²² underestimates the continuum of argon by a factor of 5. However, the total continuum energy loss rate is within a factor of two of the experimental value if $\Delta \nu = 1.5 \times 10^{15} \text{ sec}^{-1}$ is used. Using this it is found from eq. 13 that $T_a/T_e = 1.02$ in xenon, showing that the continuum radiation is not sufficient

under any circumstances to cause the electron temperature to differ appreciably from the gas temperature.

Turning now to the effect of atomic line radiation on the electron temperature, we have for the energy radiated per unit volume per second,

$$Q_{line} = \sum_j Q_j = \sum_j h \nu_j A_j N_j \quad (14)$$

where ν_j is the emission frequency, A_j the transition probability, and N_j the density of the state j . The sum over j is limited to optically thin emission lines. For strongly allowed transitions the emission probability is proportional to the square of the frequency, $A_j \approx g_j \cdot 8 \pi^2 e^2 \nu_j^2 / g_j m c^3$. The upper level, N_j , is related to the lower level by $N_j/N_l = g_j \exp(-h \nu_j / k T_e) / g_l$. If the gas is to be optically thin the lower level is limited to the value given by eq. 12 with $R_y [(n-1)^{-2} - n^{-2}]$ replaced by $h \nu_j$. Then

$$Q_j = \frac{8 \pi^2 h}{c^3} \left[\frac{2 k T}{\pi M} \right] \nu_j^4 \exp(-h \nu_j / k T_e) \quad (15)$$

It is seen that Q_j has a maximum at $h \nu_j = 4 k T_e$. Substituting this value into eq. 15 and retaining only one level, j , as representative of the sum, eq. 14 can be equated to the elastic energy transfer rate²³ to give for the temperature difference

$$\frac{T_a}{T_e} - 1 = 59 \sqrt{N k T_a / m} (k T_e)^{4.5} / h^3 c^3 e^4 N_e^2 \quad (16)$$

Using potassium at $T_e = 3000^\circ\text{K}$ as a numerical example, $T_a/T_e = 1.2$ when $N_e = 1.6 \times 10^{13} \text{ cm}^{-3}$. This is a lower limit to N_e for this temperature difference because only one line was included in the sum and also because pressure broadening may appreciably reduce the absorption coefficient.

A lowering of the electron temperature below the gas temperature under quasi-steady conditions has been reported in the shock tube measurements of excitation temperatures of chromium done by Charatis and Wilkerson.²⁴ The measured electron temperature was of the order of 6000°K for an atom temperature of $10,000^\circ\text{K}$. However, in a more recent article²⁵ Charatis and Wilkerson have revised the radiative transition probabilities used previously by computing them from their spectroscopic measurements. They now find that the electron temperature is within 3% of the gas temperature. Considerable caution must be exercised in using one experiment to show that the gas is in equilibrium and also to obtain radiative transition probabilities. Further experimental data is needed in order to determine with certainty the influence of line emission on the electron temperature. Note also that the introduction of stable molecular species will greatly increase the radiation energy loss and may lower the electron temperature significantly.

To summarize this section, the range of physical parameters for which non-equilibrium populations of excited states may occur has been determined and generally falls outside the operating range of mhd power generators, but does include the operating range of many propulsion devices. The continuum radiation has been shown to have negligible effect on the electron temperature. The range of parameters for which line radiation significantly lowers the electron temperature has been given and also generally falls outside the operating range of mhd power generators, but includes the operating range of many propulsion devices.

Nozzle Expansion and Crossed Field Accelerator

The reaction rate theory described here has been combined with two fluid one-dimensional compressible flow theory and solved on an IBM 7090 to determine the properties of argon and of helium in the deLaval nozzle expansion of the thermal arc heated gas.¹² It has also been used to compute electron density, electron temperature, electrical conductivity, gas temperature, and enthalpy in a supersonic free jet crossed field accelerator. The accelerator performance determined theoretically is in reasonable agreement with experimental measurements.¹² A few typical results are shown graphically here in Figs. 6, 7, and 8 and are discussed briefly below. For details see Ref. 12.

The degree of ionization of helium in a deLaval nozzle expansion is shown in Fig. 6. It is assumed that the gas is in equilibrium initially at the nozzle entrance. Two solutions are shown, one assuming that radiation is absorbed, the other assuming that all radiation is emitted. The electron density for the optically thin case decreases even in the nozzle entrance, tending toward the quasi-steady value of electron density for the case of optically thin helium at the stagnation temperature. Based on estimates of the absorption given above, the optically thick case is applicable to most experimental conditions. In both cases it is seen that the amount of recombination is small. It is also evident that the approximation suggested by Bray which has been successfully applied to atomic recombination²⁷ in nozzle expansions is not valid for electron-ion recombination.

Results of calculations of the properties of argon in a supersonic free jet crossed-field accelerator are shown in Figs. 7 and 8. The starting

conditions, noted in the figure, are those obtained from the nozzle computation described above and applied to argon. A step function increase in electric and magnetic field at $x = 0$ is assumed. In this calculation the effect of radiation on the reaction rates is neglected. This is not justified for hydrogenic atoms, but is for argon because of the closely spaced excited electronic levels. It has also been shown that radiation energy losses are negligible in the crossed field accelerator operating under the conditions of the computations presented here.¹² In Fig. 7 it is seen that the electron temperature rises sharply to about $16,000^{\circ}\text{K}$, followed by a region of increasing electron density. An initial dip in the electrical current is caused by an increase in the Hall parameter, due to the increase in electron temperature and corresponding decrease in cross-section. The electrical current reaches zero at the point at which the gas has been accelerated to the E/B velocity. Very little electron-ion recombination occurs in the exhaust of the accelerator because of the low electron density and high electron temperature.

Conclusions

The basis for a satisfactory electron-ion reaction rate theory has been presented and used to indicate the range of physical parameters for which significant non-equilibrium phenomena may be encountered. Illustrations of the application of the theory have been given from which it appears that the use of non-thermal ionization, that is ionization greater than the Saha equilibrium value at the electron temperature, in mhd generators is not practical; and that electron heating either by internal current or by external means in non-equilibrium mhd generators is most attractive when applied to mixtures of heavy ions and light neutrals. It was shown that the influence of line radiation on the electron temperature is significant at low electron densities although continuum radiation is not. The electron density and temperature in an arc jet nozzle expansion and a crossed field accelerator are found to be far from equilibrium which shows that a complete reaction rate theory is required in computing gas properties under these conditions.

References

1. M. Gryzinski, Phys. Rev. 115, 374 (1959).
2. J. L. Kerrebrock, "Engineering Aspects of Magnetohydrodynamics," 327, Ed. C. Manna and N. W. Mather, Columbia University Press, 1962.
3. H. Hurwitz, Jr., G. W. Sutton, S. Tamor, ARS Journal 32, 1237 (1962).
4. E. J. Sternglass, "MHD Power Generation by Nonthermal Ionization and its Application to Nuclear Energy Conversion," Third Symposium on Engineering Aspects of Magnetohydrodynamics, University of Rochester, 1962.
5. D. J. Ben Daniel, S. Tamor, Physics of Fluids 5, 500 (1962).
6. H. S. W. Massey, E. H. S. Burhop, "Electronic and Ionic Impact Phenomena," Oxford Univ. Press, London, 1952.
7. D. R. Bates, A. E. Kingston, R. W. P. McWhirter, Proc. Roy. Soc. A, 267, 297 (1962).
8. D. R. Bates, A. E. Kingston, R. W. P. McWhirter, Proc. Roy. Soc. A, 270, 155 (1962).
9. S. Byron, R. C. Stabler, P. I. Bortz, Phys. Rev. Letters 8, 376 (1962).
10. H. A. Bethe, E. E. Salpeter, Quantum Mechanics of One- and Two-Electron Atoms, Academic Press, New York, 1957.
11. F. Robben, "A Spectroscopic Study of Recombination in a Helium Plasma," 4th Annual Meeting Div. Plasma Physics, Amer. Phys. Soc., Atlantic City, November, 1962.
12. G. R. Russell, S. Byron, P. I. Bortz, "Performance and Analysis of a Non-Equilibrium Crossed Field Accelerator." AIAA Electric Propulsion Conf., Colorado Springs, March 3, 1963.
13. NBS Circular 467, "Atomic Energy Levels," U.S. Government Printing Office, Washington, D.C. (1952).
14. J. G. Baker, D. H. Menzel, Astrophys. J. 88, 52 (1938). L. C. Green, P.P. Rush, E. D. Chandler, Astrophys. J. Suppl. 3, 37 (1957).
15. L. Goldberg, Astrophys. J. 82, 1 (1935).
16. See, for example, L. H. Aller, Astrophysics, The Atmospheres of the Sun and Stars, Ronald Press, New York, 1959.

References, (Continued)

17. M. Baranger, "Spectral Line Broadening in Plasma," Chap. 13 in Atomic and Molecular Processes, Ed. D. R. Bates, Academic Press (1962).
18. H. R. Griem, Bull. Amer. Phys. Soc. II 4, 236 (1959).
19. J. Pomerantz, J. Quant. Spectrosc. Radiat. Transfer 1, 185 (1961).
20. H. N. Olsen, Phys. Rev. 124, 1703 (1961).
21. S. C. Brown, Basic Data of Plasma Physics, Technology Press and John Wiley, New York (1959).
22. H. E. Petschek, P. H. Rose, H. S. Glick, A. Kane, A. R. Kantrowitz, J. Appl. Phys. 26, 83 (1955).
23. H. Petschek, S. Byron, Annals of Physics 1, 270 (1957).
24. G. Charatis, T. D. Wilkerson, Phys. Fluids 2, 578 (1959).
25. G. Charatis, T. D. Wilkerson, Phys. Fluids 5, 1661 (1962).
26. D. J. Ben Daniel, C. M. Bishop, "Non-Equilibrium Ionization in a High Pressure Cesium-Helium Transient Discharge."
27. K. N. C. Bray, J. Fluid Mech. 6, 1 (1959).

Figure Captions

1. The function $g_j(E_2/U; E_1/U)$ used in Gryzinski's semi-classical theory of Electronic inelastic cross-sections.
2. Slope, B, of the portion of g_j that is a linear function of E_2/U .
3. The averaged product of the electron speed times the collisional de-excitation cross-section of the excited state having binding energy E^* as a function of E^* for several gases.
4. De-excitation rate of excited states normalized by the cube of the electron density as a function of the binding energy. These rates are computed assuming that the excited states are maintained in equilibrium with the free electron density by inelastic collisions.
5. Theoretical electron-ion recombination rates normalized by the cube of the electron density for several gases.
6. Degree of ionization of helium in a deLaval nozzle expansion from a thermal arc.
7. Gas properties of argon in a supersonic free jet crossed field accelerator using a constant pressure two fluid non-equilibrium compressible flow theory.
8. Gas properties of argon in a supersonic free jet crossed field accelerator using a constant pressure two fluid non-equilibrium compressible flow theory.

